**Proceedings of the ASME 2009 International Design Engineering Technical Conferences &
Computers and Information in Engineering Conference
IDETC/CIE 2009
August 30 - September 2, 2009, San Diego, California, USA**

DETC2009-86987

TRAJECTORY REAL-TIME OBSTACLE AVOIDANCE FOR UNDERACTUATED UNMANNED SURFACE VESSELS

Reza A. Soltan, Hashem Ashrafiuon*, and Kenneth R. Muske
Center for Nonlinear Dynamics and Control,
Villanova University, Villanova, PA, 19085
* Corresponding Author, Email: hashem.ashrafiuon@villanova.edu

ABSTRACT

A new method for obstacle avoidance of underactuated unmanned surface vessels is presented which combines trajectory planning with real-time tracking control. In this method, obstacles are approximated and enclosed by elliptic shapes which represent the stable limit cycle solution of a special class of ODEs (ordinary differential equation). The vessel trajectory at any moment is defined by the ODEs whose solution is the limit cycle defining the obstacle immediately on its path to the target. When no obstacle remains on the vessel's path, the trajectory is defined by exponentially stable ODEs whose solution is the target trajectory. The planned trajectories are tracked by the vessel through a sliding mode control law which is robust to environmental disturbances and modeling uncertainties and can be computed in real time. One advantage of the method is that it allows for dynamic (moving and rotating) obstacles as well as a moving target. Another advantage is that only the current information about the obstacles and the target are required for real-time trajectory planning. Since the vessel current position is used as feedback to redefine the limit cycle trajectories, the method is also robust to large disturbance.

INTRODUCTION

Autonomous surface vessels with two actuator inputs are considered as underactuated mechanical systems since they posses three DOF when modeled as a single planar rigid body. Nonlinear position control of underactuated vehicle systems is an interesting and complex research topic due to modeling uncertainties, underactuation, and only indirect control of tracking variables through non-holonomic constraints. For example, consider the planer model of a surface vessel shown in Fig. 1. The control inputs from the two propellers can only provide a surge motion and planar rotation. The difficulty arises from the fact that only one input (total surge force) will appear in the two nonlinear differential equations representing the horizontal and vertical motion. Hence, tracking a path or trajectory is only possible with the aid of the yaw rotation. Hence, the mathematical formulation of the control problem is not trivial. In general, tracking control may

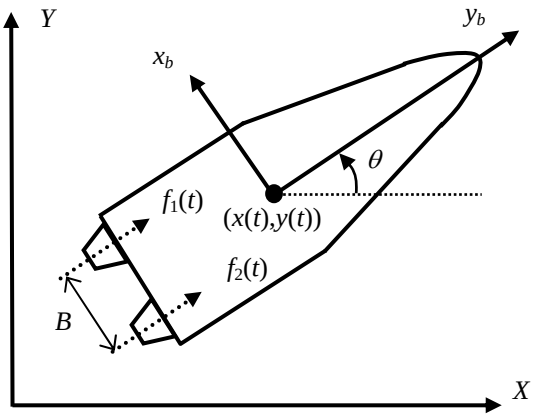

Figure 1. Planar model of a surface vessel

only be possible if the trajectory to be followed does not include all three position variables simultaneously. For example, in the case of the surface vessel shown in Fig. 1, only position can be tracked precisely while the heading angle is uncontrolled, i.e. the desired trajectory does not include a desired heading angle [1-5].

Recently the Naval scientists have been involved in the development of obstacle avoidance for USV (unmanned surface vessels) to achieve a high level of autonomous navigation. An autonomous USV can fulfill a variety of missions and applications that are of increasing interest. The USV obstacle avoidance algorithm is being developed first by accurately creating a world model based on various sensors such as vision, radar, and nautical charts. Using this world model the USV can avoid obstacles with the use of a far-field deliberative obstacle avoidance component and a near-field reactive obstacle avoidance component. More specifically, the current focus is to create a robust obstacle avoidance capability and then move on to more advanced behaviors such as autonomous recovery in the case of lost communications, target tracking and/or interception, collaborative behaviors [6].

However, the literature for obstacle avoidance for mobile robot is richer due to the typical lower speed and lower orders of constraint. Much of the work in this field is focused on trajectory optimization and partially open-loop model predictive control. Since finding the desired trajectory and calculating the control action is normally too time-consuming, many of these works are not recommended for real-time controllers, especially in the presence of disturbances [7-9]. As a result, decentralized control approach has been proposed to achieve more robustness and to reduce communication along the robots/agents. In the decentralized control approaches (including hybrid control algorithms), local control laws are defined for each robot based on local information [10-13]. Behavior-based approach has also been introduced to simplify the definition of control laws in the decentralized control approach [14, 15]. A very promising and well researched approach to obstacle avoidance is the potential field method, which has been extensively utilized for mobile robots with static and dynamic obstacles [16-23].

Limit cycles have been previously used to generate trajectories for robots in order to avoid obstacles [24]. In their work, the authors define unstable limit cycles as objects of finite size and shape, as a way of modeling complex obstacles to be avoided. Application of real-time navigation method for mobile robots using limit cycles has also been addressed by a few researchers [25-27]. However, these works do not address the development of a stable and robust control law. In addition, the limit cycles are defined as simple stationary circular ones [28, 29], which may result in impractical control demand depending on the distance of the vehicle to the obstacle. In other words, using constant coefficients in the limit cycle equations applies only to stationary obstacles and may require unreasonably high velocities when the robot is too far from the limit cycle. There are, however, other works which use more sophisticated controllers for real time tracking and formation control of mobile robots but do not take advantage of limit cycle based trajectories [30-32].

In this work, we present a novel obstacle avoidance method for underactuated USVs based on a nonlinear sliding mode control [33-35]. The USV trajectory is defined as a set of two ODEs in terms of the two planar global position variables where the vessel position feedback is continually used to redefine the trajectory and add robustness when unaccounted disturbance is present. At each sample time, the obstacles on the straight line path of the USV to its target are detected and the vessel targets the nearest obstacle on its path. Hence, a transitional trajectory is defined through a set of two ODEs whose solution is a stable limit cycle in the shape of an ellipse approximating and enclosing the target obstacle. If the obstacle at any time moves of the way or when the USV goes around the obstacle, the trajectory is then switched to another limit cycle approximating and enclosing the next obstacle on the USV path to its ultimate target. This process continues until all obstacles are cleared. The final transition trajectory is then defined by a set of two exponentially convergent ODE's whose solution is the target trajectory. During each transitional trajectory, an asymptotically stable sliding mode control law for the underactuated USV [34] guarantees convergence. The stability of the moving and reorienting elliptical limit cycles can also be established using previously developed techniques [36]. Two simulation examples are presented for a USV catching a moving target in presence of several moving and reorienting obstacles.

TRAJECTORY PLANNING STRATEGY

Consider the following information are available at the current time: the vessel's global position, $x(t)$ and $y(t)$, the vessel orientation, $\theta(t)$, the target's global position, $x_t(t)$ and $y_t(t)$, and the obstacles' enlarged approximate sizes and locations as listed in Table 1.

Table 1. Required Obstacle data for i = 1 to n

	Description
n	The number of obstacles
$x_{obs}(i,t)$	Current position of the center of the obstacles in the global x direction at any instant of time
$y_{obs}(i,t)$	Current position of the center of the obstacles in the global y direction at any instant of time
$a(i)$	Semi-major axis of the ellipse, surrounding the obstacles
$b(i)$	Semi-minor axis of the ellipse, surrounding the obstacles
$\varphi(i,t)$	The current orientation angle of the ellipse, surrounding the obstacles at any instant of time

The strategy is based on approximating all obstacles as ellipses and defining ODE's whose solutions are stable elliptical limit cycles representing the obstacles. As the first step we assume that the best solution to reach the target is a straight line from the vessel to the target. We then find the intersections of this line with the nearest obstacle and choose the limit cycle representing that obstacle as the desired trajectory. This process is then repeated for all subsequent obstacles on the way of the vessel to the target which results in switching from one limit cycle to another. When there are no obstacles on the vessel's path to the target, an exponentially stable desired trajectory is selected to catch the target.

The *limit cycle trajectory* may be defined by the following set of ODE's for a planar trajectory:

$$\begin{cases} \dot{x}_1(t,i) = +sw(i)\omega(i)x_2(t,i) - a_1(t,i)x_1(t,i)[g(t,i)] \\ \dot{x}_2(t,i) = -sw(i)\omega(i)x_1(t,i) - a_2(t,i)x_2(t,i)[g(t,i)] \end{cases} \quad (1)$$

where $x_1(t,i) = x(t) - x_{obs}(i,t)$ and $x_2(t,i) = y(t) - y_{obs}(i,t)$ are the state variables of the trajectory and $g(t,i)$ is the equation of the elliptical limit cycles around obstacle i:

$$g(t,i) = [\cos\varphi(i,t)x_1(t,i) + \sin\varphi(i,t)\, x_2(t,i)\,]^2/a(i)^2 + [-\sin\varphi(i,t)\, x_1(t,i) + \cos\varphi(i,t)\, x_2(t,i)]^2/b(i)^2 - 1 = 0 \quad (2)$$

It is clear that if two or more obstacles collide or are too close to each other, they can be approximated and enclosed by a one larger ellipse. The variable $sw(i)$ can be either +1 or −1, such that +1 leads to USV counterclockwise and −1 leads to clockwise motion around limit cycle i and $\omega(i)$ is the positive angular velocity of the USV on the limit cycle, which is selected based on the size of the limit cycle to keep the absolute velocity of the USV within its physical limit. The coefficients $a_1(t,i)$ and $a_2(t,i)$ are positive functions inversely related to the distance between the USV and the limit cycle in the two planar directions to avoid large unfeasible velocity requirements.

The *final trajectory* is generated in order to catch the target by solving the exponentially stable ODE's as follows:

$$\begin{cases} \dot{x}_1(t) = -k_1(t)x_1(t) & , k_1(t) > 0 \\ \dot{x}_2(t) = -k_2(t)x_2(t) & , k_2(t) > 0 \end{cases} \quad (3)$$

where $x_1(t) = x(t) - x_t(t)$ and $x_2(t) = y(t) - y_t(t)$, and $k_1(t)$ and $k_2(t)$ are positive functions, defined based on the distance between the USV and the target.

Let us explain the algorithm which finds the obstacles, defines the *limit cycle trajectories* and the *final trajectory* and how it switches from one trajectory to the next in order to avoid the obstacles and catch the target:

Step 1. The obstacles on the USV path to the target are identified using the intersection points between the straight line from the USV to the target and the elliptical limit cycles. The equation of the straight line $L(t)$ is given by:

$$L(t):\ Y(t) - y_t(t) = (X(t) - x_t(t))\ (y(t) - y_t(t))\ /\ (x(t) - x_t(t)) \quad (4)$$

where $X(t)$ and $Y(t)$ are the two variables of the planar straight line. All obstacles which do not have any intersection with the straight line are ignored at the present time.

Step 2. The algorithm sorts the limit cycles based on their distances to the USV finds the nearest obstacle. It then generates the *limit cycle trajectory* of Eq. (2) based on the size, orientation, and location of the obstacle. The value of the switching variable "*sw*" is selected based on the shortest path around the obstacle toward the target which can be easily identified using the location of the intersection points with respect to the center if the ellipse.

Step 3. The USV tracks the current trajectory while the calculation of steps 1 and 2 are repeated until a new obstacle is identified. The USV then switches to the new trajectory defined for the new obstacle.

Step 4. When all obstacles are cleared, the *final trajectory* of Eq. (3) is used to catch the target. Note that, the check in step (1) is continually repeated such that if obstacles move to block the USV path, the algorithm reverts back to steps (2) and (3).

CONTROLLER DESIGN

In the most general case, the desired state trajectory is described by a nonlinear dynamic system as follows:

$$\dot{x}_i(t) = h_i(x_1(t), x_2(t)), \;\; h_i : \mathbf{S}_i \rightarrow \mathbf{R}^2, \;\; i = 1,2 \tag{5}$$

where $x_1(t)$ and $x_2(t)$ are the state variables of the desired trajectory, $\mathbf{S}_i$ is an open and connected subset of $\mathbf{R}^2$, and h_i is a locally Lipschitz map from $\mathbf{S}_i$ into $\mathbf{R}^2$. Equations (1) and (3) are subsets of Eq. (5). The difficulty arises in the USV control arises from the fact that the state variables of the desired trajectory are not directly controlled but are related to controlled variables through non-holonomic constraints as explained below.

In order to develop the control forces, we use the nonlinear differential equations of motion of the USV in the body-fixed reference frame as:

$$\begin{aligned} & m_{11}\dot{v}_x(t) - m_{22}v_y(t)\omega(t) + d_{11}v_x^{\alpha_1}(t) = f(t) \\ & m_{22}\dot{v}_y(t) + m_{11}v_x(t)\omega(t) + d_{22}\,\mathrm{sgn}(v_y(t))\left|v_y(t)\right|^{\alpha_2} = 0 \\ & m_{33}\dot{\omega}(t) + m_d v_x(t)v_y(t) + d_{33}\,\mathrm{sgn}(\omega(t))\left|\omega(t)\right|^{\alpha_3} = T(t) \end{aligned} \tag{6}$$

where $v_x(t)$ and $v_y(t)$ are the vessel's forward and lateral velocities, $\omega(t)$ is the angular velocity, and $m_d = m_{22} - m_{11}$ and $m_{22} \neq m_{11}$. Note that only forward motion dynamics are considered. The surge force $f(t)$ and the yaw moment $T(t)$ are derived in terms of the two propeller $f_1(t)$ and $f_2(t)$ as: $f = f_1 + f_2$ and $T = (f_2 - f_1)/2\mathrm{B}$. For details regarding the parameters m_{ii}, d_{ii}, α_i, i=1,2,3, the reader is referred to [1] and [37].

The body-fixed reference frame velocities are related to global velocities as follows:

$$\begin{aligned} & \dot{x}(t) = v_x(t)\cos\theta(t) - v_y(t)\sin\theta(t) \\ & \dot{y}(t) = v_x(t)\sin\theta(t) + v_y(t)\cos\theta(t) \\ & \dot{\theta}(t) = \omega(t) \end{aligned} \tag{7}$$

where $\dot{x}(t)$, $\dot{y}(t)$, and $\dot{\theta}(t)$ are global linear and angular velocities. More details on the USV model derivation and relations are presented in [1] and [34].

The control law developed for this work is based on the sliding mode approach [38, 39] where a set of asymptotically stable surfaces (S) are defined as a function of the tracking errors such that all system trajectories converge to these surfaces in finite time and slide along them until they reach the desired destination at their intersection [28]. The reaching conditions are established by defining $\frac{1}{2}S^T S$ as a Lyapunov function and ensuring that for surface i:

$$S_i\dot{S}_i \leq -\eta_i\left|S_i\right|, \;\; \eta_i > 0 \tag{8}$$

where the value of the constants η_i (effort parameters) determine how fast the trajectory will reach surface i.

In the case of underactuated surface vessels, two surfaces in terms of the surge and lateral velocities are defined to determine the two control inputs. The desired state trajectories in the inertial reference frame are related to the desired surge and lateral velocity and acceleration as:

$$\begin{aligned} & v_{xd}(t) = \cos\theta(t)\,\dot{x}_1(t) + \sin\theta(t)\,\dot{x}_2(t) \\ & \dot{v}_{xd}(t) = \cos\theta(t)\,\ddot{x}_1(t) + \sin\theta(t)\,\ddot{x}_2(t) + v_{yd}(t)\omega(t) \end{aligned} \tag{9a}$$

$$\begin{aligned} & v_{yd}(t) = -\sin\theta(t)\,\dot{x}_1(t) + \cos\theta(t)\,\dot{x}_2(t) \\ & \dot{v}_{yd}(t) = -\sin\theta(t)\,\ddot{x}_1(t) + \cos\theta(t)\,\ddot{x}_2(t) - v_{xd}(t)\omega(t) \end{aligned} \tag{9b}$$

Surge Control Law

The first sliding surface is a first order one, defined in terms of the vessel's surge motion tracking error

$$S_1(\tilde{v}_x) = \tilde{v}_x(t) + \lambda_1\int_0^t \tilde{v}_x(\tau)d\tau \tag{10}$$

where "~" is used to denote the tracking errors which is the difference between the actual and desired values; i.e. $\tilde{v}_x(t) = v_x(t) - v_{xd}(t)$. Note that $v_{xd}(t)$ is expressed in terms of $\dot{x}_1(t)$ and $\dot{x}_2(t)$, as shown in Eq. (9a). The values of $\dot{x}_1(t)$ and $\dot{x}_2(t)$ can either be computed from a desired state trajectory $\dot{x}_d(t)$ and $\dot{y}_d(t)$ as proposed in the reference [34], or from Eq. (5) in terms of the state position feedbacks: $x(t)$ and $y(t)$.

Taking the time derivative of the surface and using the first relationship in Eq. (9a), the surge control input can be determined as:

$$f(t) = f_s(t) - k_s(t)\,\mathrm{sgn}(S_1(\tilde{v}_x(t))) \tag{11}$$

where the terms

$$f_s(t) \equiv f_s(v_x(t), v_y(t), \omega(t), v_{xd}(t), \dot{v}_{xd}(t)) \tag{12a}$$

$$k_s(t) \equiv k_s(v_x(t), v_y(t), \omega(t), v_{xd}(t), \dot{v}_{xd}(t)) \tag{12b}$$

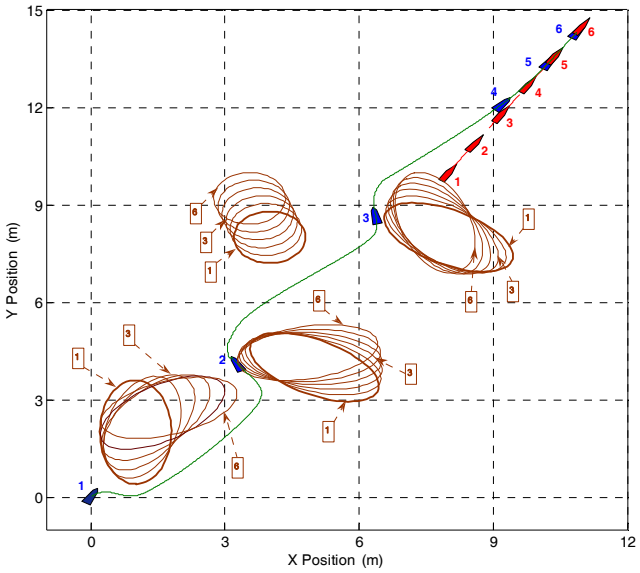

Figure 2. USV catching a moving target through dynamic obstacles during the first scenario

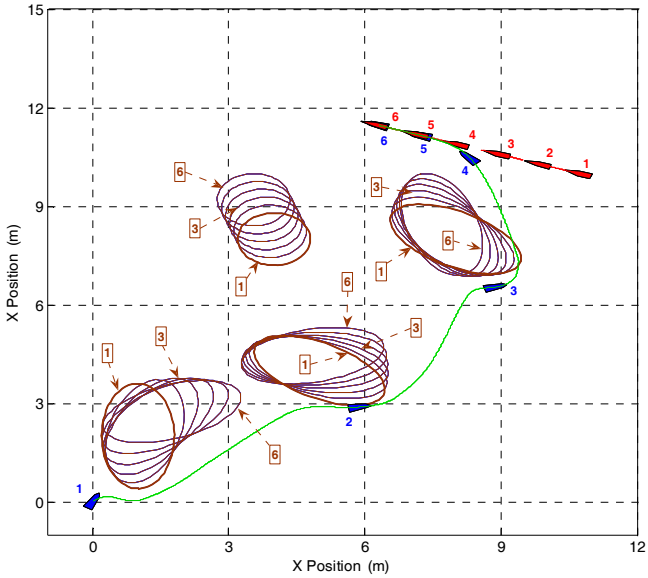

Figure 3. USV catching a moving target through dynamic obstacles during the second scenario

are derived based on the nominal model and its uncertainty bounds as presented in [34]. Note that, the wave and wind forces may also be modeled [1] with their uncertainties and accounted for in Eq. (11).

Lateral Motion Control Law

We define the second sliding surface as a second-order one in terms of the vessel's lateral motion tracking errors

$$S_2(\tilde{v}_y, \dot{\tilde{v}}_y) = \dot{\tilde{v}}_y(t) + 2\lambda_2 \tilde{v}_y(t) + (\lambda_2)^2 \int_0^t \tilde{v}_y(\tau) d\tau \qquad (13)$$

where $\tilde{v}_y(t) = v_y(t) - v_{yd}(t)$ & $\dot{\tilde{v}}_y(t) = \dot{v}_y(t) - \dot{v}_{yd}(t)$. The derivation of the time derivative of the second surface requires $\ddot{v}_y(t)$. Hence, taking the time derivative of the lateral equation of motion in Eq. (6) and substituting for the accelerations from the surge and yaw equations, the yaw moment control can be calculated. The yaw control moment is derived as a function of the surge control force as:

$$T(t) = f_y(t) - k_y(t)\,\mathrm{sgn}(S_2(\tilde{v}_y(t), \dot{\tilde{v}}_y(t))) \qquad (14)$$

where the terms

$$f_y(t) \equiv f_y(v_x(t), v_y(t), \omega(t), v_{xd}(t), v_{yd}(t), \dot{v}_{xd}(t), \dot{v}_{yd}(t), \ddot{v}_{yd}(t), f(t)) \qquad (15)$$

$$k_y(t) \equiv k_y(v_x(t), v_y(t), \omega(t), v_{xd}(t), v_{yd}(t), \dot{v}_{xd}(t), \dot{v}_{yd}(t), \ddot{v}_{yd}(t), f(t)) \qquad (16)$$

are derived based on the nominal model and its uncertainty bounds as presented in [34]. Again, note that the wave and wind moments may also be modeled and their uncertainties can be accounted for in Eq. (14) through these terms.

SIMULATIONS

The USV model used in simulations has the following data in SI units shown in the Table 2 [37]:

Table 2. The USV model parameters in SI units

$m_{11} = 1.956$	$m_{22} = 2.405$	$m_{33} = .043$
$d_1 = 2.436$	$d_2 = 12.992$	$d_3 = .0564$
$\alpha_1 = 1.510$	$\alpha_2 = 1.747$	$\alpha_3 = 1.592$

We consider two different constant velocity-straight line target trajectories for our example. The coordinates of the moving target in the first scenario are defined as:

$$x_t(t) = (0.03)\,t + 8, \quad y_t(t) = (0.03)\,t + 10 \qquad (17)$$

While the coordinates of the moving target in the second scenario are given as:

$$x_t(t) = (-0.02)\,t + 11, \quad y_t(t) = (0.01)\,t + 10 \qquad (18)$$

There are four obstacles which are assumed to be moving at constant speed and also rotating at constant angular velocity. The obstacle data are presented in Table 3.

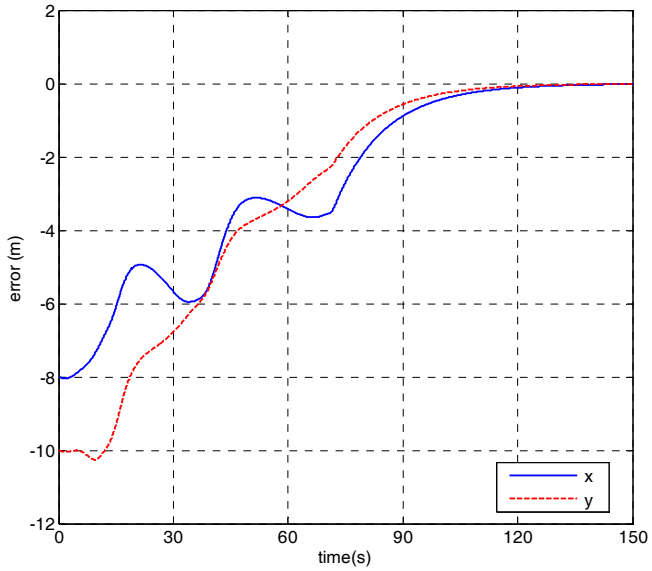

Figure 4. The trajectory error in x and y directions for the first scenario

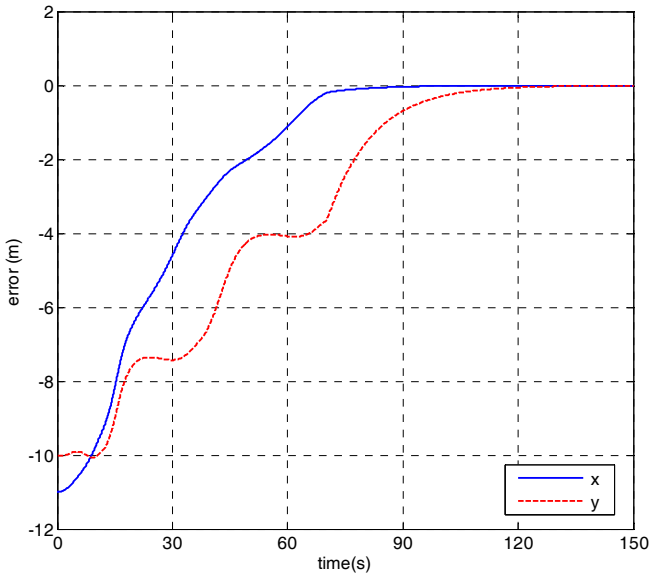

Figure 5. The trajectory error in x and y directions for the second scenario

Table 3. Obstacle size, position, and motion data

	Obstacle #1	Obstacle #2	Obstacle #3	Obstacle #4
x_{obs}	8	5	4	1
dx_{obs}/dt	-0.002	-0.001	-0.003	0.005
y_{obs}	8	4	8	2
dy_{obs}/dt	0.003	0.003	-0.008	0.005
a	2	2	1	2
b	1	1	1	1
φ_{obs}	-π/6	-π/6	0	π/2
$d\varphi_{obs}/dt$	-0.005	0.005	0.008	-0.008

The control parameters are selected as $\eta_1 = 1$, $\eta_2 = 1$, and $\lambda_1 = \lambda_2 = 2$. However, the effort parameters may need to be adjusted according to the actuator limits. The discontinuous "sign" functions were also replaced with continuous saturation functions of boundary layer thicknesses $\phi_1 = \phi_2 = .1$ [29].

The simulations were run for 150 seconds for both scenarios and partial frame by frame results are displayed in Figures 2 and 3 where the USV is clearly able to catch the target while passing safely through the field of moving obstacles. In these figures, we have displayed six different frames, one every 30 seconds including the initial frame. Hence, the indicators 1 through 6 represent the objects at times t = 0, 30, 60, 90, 120, 150 s. Figures 4 and 5 show the global position trajectory errors between the USV and the target for the two scenarios. Note the smooth convergence of the trajectories with occasional "bumps" due to obstacle interference.

Figures 6 and 7 show the control forces for the left and right motors (i.e. $f_1(t)$ and $f_2(t)$) to accomplish the mission for the first and second scenario, respectively. We have only shown the first 100 seconds of simulation for clarity. Both left and right forces converge to their steady state value to keep the velocity of the USV equal to the target's constant velocity when the target is reached. These figures also show that there are large discontinuities in the control law when the USV switches from one trajectory to another. Since vessel propellers are not able to produce such discontinuities, the method may not be ready for practical implementation yet

CONCLUSIONS

A new method for obstacle avoidance and concurrent trajectory planning and tracking of USV was presented. The method plans trajectories around obstacles using ODE's whose stable limit cycle solutions approximate and enclose the dynamic obstacles. A procedure was also introduced to continuously detect obstacles and plan and track trajectories around them until the target is reached. The tracking control law that guarantees convergence and robustness was based on nonlinear sliding mode control which has been shown to be suitable for real-time implementation. Successful simulations verified the approach can be very effective for catching dynamic obstacles through a field of dynamic obstacles. However, currently large control discontinuities exist which we intend to eliminate in future work.

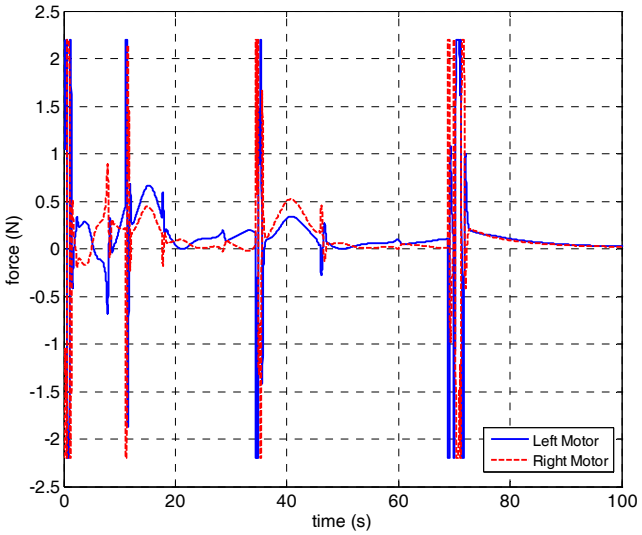

Figure 6. The control forces for the left and right motors to accomplish the mission shown for the first scenario

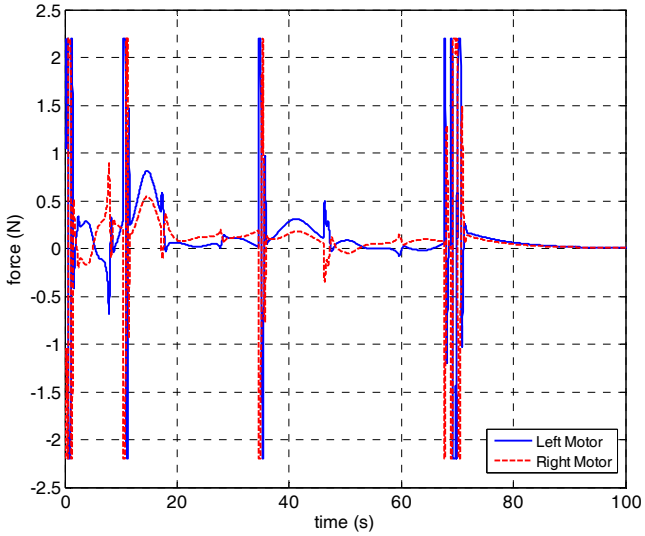

Figure 7. The control forces for the left and right motors to accomplish the mission shown for the second scenario

ACKNOWLEDGEMENTS

This research was partially supported by the Office of Naval Research under the ONR Grant number N00014-04-1-0642. Support for this work from the Center for Nonlinear Dynamics and Control (CENDAC) at Villanova University is also acknowledged.

REFERENCES

[1] Fossen, T. I., 1994, "Guidance and control of ocean vehicles," John Wiley & Sons, New York, NY.

[2] Reyhanoglu, M., 1997, "Exponential stabilization of an underactuated autonomous surface vessel," Automatica, **33** (12), pp. 2249-2254.

[3] Mazenc, F., Pettersen, K., and Nijmeijer, H., 2002, "Global uniform asymptotic stabilization of an underactuated surface vessel," *IEEE Transactions on Automatic Contro*l, **47** (10), pp. 1759-1762.

[4] Dong, W., and Guo, Y, 2005, "Global time-varying stabilization of underactuated surface vessel," *IEEE Transactions on Automatic Control*, **50** (6), pp. 859-864.

[5] Peterson, K.Y., Mazenc, F., and Nijmeijer, H., 2004, "Global Uniform Asymptotic Stabilization of an Underactuated Surface Vessel: Experimental Results," *IEEE Transactions on Control Systems Technology*, **12** (6), pp. 891-903.

[6] Larson, J., Bruch, M., Haiterman, R., Rogers, J., Webster, R., 2007, "Advances in Autonomous Obstacle Avoidance for Unmanned Surface Vehicles," AUVSI Unmanned Systems North America, Washington, DC.

[7] Elfes, A., 1989, "Using occupancy grid for mobile robot perception and navigation," Computer, **22** (6), pp. 46-57.

[8] Aggarwal, N., Fujimura, K., 1994, "Motion planning amidst planar moving obstacles," IEEE International Conference on Robotics and Automation, San Diego, CA, **3**, pp. 2153-2158.

[9] Fujimura, K., Samet, H., 1989, "A hierarchical strategy for path planning among moving obstacles," IEEE Transaction on Robotics and Automation, **5** (1), pp. 61-69.

[10] Lawton, R. J., Young, B. J., Beard, R. W., 2000, "A Decentralized Approach to Elementary Formation Maneuvers," IEEE International Conference on Robotics and Automation, San Francisco, CA, **1**, pp. 2728-2743.

[11] Yamaguchi, H., 1999 "A cooperative hunting behavior by mobile robot troops," International Journal of Robotics, **18** (9)**,** pp. 931-940.

[12] Shao, J., Xie, G., Yu, J., Wang, L., 2005, "Leader-Following Formation Control of Multiple

Mobile Robots," IEEE International Symposium on Intelligent Control, ISAC, and the 13th Mediterranean Conference on Control and Automation, Limassol, Cyprus, pp. 808-813.

[13] Sugar, T., Kumar, V., 1998, "Decentralized control of cooperating mobile manipulators," *IEEE international conference on Robotics and Automation*, Leuven, Belgium, pp. 2864-2869.

[14] Balch, T., Arkin, R.C., 1998 "Behavior-based formation control for multi robot team," IEEE Transaction on Robotics and Automation, **14** (6), pp. 926-939.

[15] Cao, Z., Xie, B., Zhang, S., Wang, S., Tan, M., 2003, "Formation Constrained Multi-Robot System in Unknown Environment," IEEE International Conference on Robotics and Automation, **1**, pp. 735-740.

[16] Warren, C., 1990, "Multiple Robot Path Coordination Using Artificial Potential Fields," *Proceedings of the IEEE International Conference on Robotics and Automation*, Cincinnati, OH, **1**, pp. 500–505.

[17] Marchese F. M., Negro, M. D., 2006, "Path Planning for multiple Generic- Shaped Mobile Robots with MCA," Lecture Notes in Computer Science, **3993**, pp. 264-271.

[18] Yun, X., and Tan, K., 1997, "Wall-Following Method for Escaping Local Minima in Potential Field Based Motion Planning," *Proceeding of the 8th International Conference on Advanced Robotics*, Monterey, CA, pp. 421– 426.

[19] Cosio, F. A., and Castaneda, M. P., 2004, "Autonomous robot navigation using adaptive potential fields," *Mathematical and Computer Modelling*, **40** (9–10), pp. 1141–1156.

[20] Ge, S. S., and Cui, Y. J., 2002, "Dynamic motion planning for mobile robots using potential field method," *Autonomous Robots*, **1**, 207–222.

[21] Fahimi, F., Nataraj, C., Ashrafiuon, H., 2009, "Real-time obstacle avoidance for multiple mobile robots", *Robotica*, **27** (2), pp. 189-198.

[22] Kim, D. H., Wang, H. O., Ye, G., and Shin, S., 2004, "Decentralized Control of Autonomous Swarm Systems using Artificial Potential Functions: Analytical Design Guidelines," *Proceedings of the IEEE Conference on Decision and Control*, Nassau, Bahamas, **1**, pp. 159–164.

[23] Kim, J., and Khosla, P. K., 1992, "Real-time obstacle avoidance using harmonic potential functions," *IEEE Transaction on Robotics and Automation*, **3**, pp. 338–349.

[24] Ellekilde, L. P., Perram, J. W., 2005, "Tool Center Trajectory Planning for Industrial Robot Manipulators Using Dynamical Systems," The International Journal of Robotics Research, **24** (5), pp.385-396.

[25] Kim, D. H., Kim, J. H., 2003, "A real-time limit-cycle navigation method for fast mobile robots and its application to robot soccer," Robotics and Autonomous Systems, **42** (1) pp.17-30.

[26] Kim, D., Chongkug, P., 2008, "Limit cycle navigation method for mobile robot," 27th Chinese Control Conference, Kunming, Yunnan, China, pp. 320-324.

[27] Grech, R., Fabri, S. G., 2005, "Trajectory Tracking in the Presence of Obstacles using the Limit Cycle Navigation Method," *IEEE International Symposium on Intelligent Control* and *the 13th Mediterranean Conference on Control and Automatio*n, Limassol, Cyprus, pp. 101-106.

[28] Slotine, J.-J. E., and Li, W., 1991, "Applied Nonlinear Control," Englewood Cliffs, NJ: Prentice Hall,

[29] Khalil, H. K., 1996, "*Nonlinear Systems"*. Prentice-Hall, Upper Saddle River, NJ, pp. 552-579.

[30] Yannier, S., Sabanovic, A., Onat, A., Bastan, M., 2005, "Sliding mode based obstacle avoidance and target tracking for mobile robot," IEEE International Symposium on Industrial Electronics, Dubrovnik, Croatia, pp. 1489-1494.

[31] Defoort, M, Floquet, T., Kokosy, A., Perruquetti, W., 2008, "Sliding mode formation control for cooperative autonomous mobile robots," *IEEE Transactions on Industrial Electronics SS on Sliding Mode Control in Industrial Applications*, **55** (11), pp 3944-3953.

[32] Sanchez, J., Fierro, R., 2003, "Sliding mode control for robot formations," *International Symposium on Intelligent Control,* pp. 438-443.

[33] Muske, K., Ashrafiuon, H., and Nikkhah, M., 2007, "A Predictive and Sliding Mode Cascade Controller," *American Control Conference*, New York, NY, pp. 4540-4545.

[34] Ashrafiuon, H., Muske, K. R., McNinch, L., and Soltan, R., 2008, "Sliding Model Tracking Control of Surface Vessels," *IEEE Transactions on Industrial Electronics*, **55** (11), pp. 4004-4012.

[35] Soltan, R. A., Ashrafiuon, H., Muske, K. R., 2009, "State-Dependent Trajectory Planning and Tracking Control of Unmanned Surface Vessels," Accepted for presentation in the American Control Conference, St. Louis, MO.

[36] Ghaffari, A., Tomizuka, M., Soltan, R. A., 2008, "The stability of limit cycles in nonlinear systems," *Nonlinear Dynamics*, DOI: 10.1007/s11071-008-9398-3.

[37] Muske, K., Ashrafiuon, H., Haas, G., McCloskey, R., and Flynn, T., 2008, "Identification of a Control Oriented Nonlinear Dynamic USV Model," *American Control Conference*, Seattle, WA, pp. 562-567.

[38] Utkin, V. I., 1977, "Variable structure systems with sliding modes," *IEEE Transactions on Automatic Control*, **22**, pp. 212-222.

[39] Hung, J. Y., Gao, W., Hun, J. C., 1993, "Variable structure control: A survey," IEEE Trans. Ind. Electron., **40** (1), pp. 2-22.